Scientific paper

Spectroscopic Signatures of $[H_9O_4]^+$ and $[H_{13}O_6]^+$ Ions in a Polar Aprotic Environment Revealed Under DFT-PCM Approximation

Mikhail V. Vener,[1,*] Shushu Kong,[2] Alla A. Levina[1] and Ilya G. Shenderovich[2,3]

[1] *Department of Quantum Chemistry, Mendeleev University of Chemical Technology, Miusskaya Square 9, 125047 Moscow, Russia*

[2] *Institut für Chemie und Biochemie, Freie Universität Berlin, Takustrasse 3, D-14195 Berlin, Germany*

[3] *Department of Physics, St. Petersburg State University, 198504, St. Petersburg, Russia*

* *Corresponding author: E-mail: mikhail.vener@gmail.com*

Received: 15-03-2011

Dedicated to Professor Dušan Hadži on the occasion of his 90th birthday

Abstract

The structures, relative stability, infrared (IR) and Raman spectra of the most-stable forms of $[H_9O_4]^+$ and $[H_{13}O_6]^+$ ions in acetonitrile are computed using the B3LYP functional combined with the Polarizable Continuum Model approximation. These forms are hydrated $[H_3O]^+$ and $[H_5O_2]^+$ cores. Of interest are two main environmental effects on the spectroscopic features of protonated water hydrates: (i) polarization of the solvent by the hydrate dipole moment; (ii) formation of H-bonds with bulky counterions (ClO_4^- and BF_4^-). The effect of the polarization on the structure of the $[H_3O]^+$ core strongly depends on the symmetry of the hydration shell. A distortion of a hydrated $[H_3O]^+$ easily changes its structure to the $[H_7O_3]^+$ one that causes a change in the nature of the most IR-intensive bands. Thus, the specificity of this core can be easily lost that prevents identification of the corresponding species. By contrast, the $[H_5O_2]^+$ core is more stable against distortion. It is characterized by the short O…O distance (< 2.45 Å), IR-intensive band near 1720 cm^{-1} and Raman-intensive line around 500 cm^{-1}. The $[H_5O_2]^+$ core remains identifiable even when protonated hydrate is involved in specific interactions with a bulky counterion. Geometrical criteria for identification of the $[H_3O]^+$, $[H_5O_2]^+$ and $[H_7O_3]^+$ cores are discussed.

Keywords: B3LYP-PCM computations, protonated water hydrates, bulky counterions

1. Introduction

During the last two decades a great attention has been paid to the structure of protonated water hydrates in the gas and condensed phases.[1–11] Different experimental[1–3, 12–19] and theoretical studies[6,20–28] led to valuable insight into spectroscopic features and proton dynamics in the gas-phase hydrates. DFT based MD simulations of proton transfer in acidic solvents[29–40] clarified several important issues, however, the spectroscopic signatures of different protonated water hydrates in liquid state have not been revealed yet. This is due to technical limitations of the DFT based MD simulations of acidic solvents[29] and difficulties in experimental identification of the simplest stable protonated water hydrates in the liquid state.[9,10] The gas-phase studies of the considered clusters are of limited applicability to acidic solvents due to the absence of environmental effects and a counterion. DFT computations of molecular crystals and periodic systems give some hints into the proton dynamics, however, the size of the protonated water hydrates is defined by the initial conditions and is usually limited to the protonated water tetramer.[7,41] It should be noted that the results of the DFT based MD simulations of the excess proton in water depend strongly on the particular semi-local functional used in the calcula-

tions.[29,33,35] Moreover, these simulations are usually performed without a counterion.

In the present study we compute the structures, relative stability, infrared (IR) and Raman spectra of the most-stable forms of $[H_9O_4]^+$ and $[H_{13}O_6]^+$ ions in a polar aprotic environment using the B3LYP functional combined with the Polarizable Continuum Model approximation (B3LYP-PCM). These ions are selected due to the following reasons. The two most stable forms of an isolated $[H_9O_4]^+$ ion in the gas phase are a partially hydrated $[H_5O_2]^+$ core, that is $[H_5O_2]^+(2H_2O)$, and a fully hydrated $[H_3O]^+$ core, that is $[H_3O]^+(3H_2O)$. The latter is often called as the Eigen-ion. A dynamic equilibrium between these two forms was studied in the gas-phase.[21–23,25] These two forms are generally assumed to be the most suitable model species feasible to describe proton solvation in acidic solvents.[29–40] However, some other experimental data suggest that under specific conditions the proton is solvated as a $[H_{13}O_6]^+$ cluster [10]. In the gas phase this cluster exist either as a fully hydrated $[H_5O_2]^+$ core, that is $[H_5O_2]^+(4H_2O)$ or as a distorted $[H_3O]^+$ core, that is $[H_3O]^+(5H_2O)$.[25] Thus, it is of crucial importance to identify experimental criteria feasible to discriminate between different proton solvation structures, as it has been done in the past for systems with proton transfer.[42] In the case of success it will provide a background to determine proton solvation structures in amorphous systems.[43,44]

The specific aims of this study are: (i) to identify spectroscopic signatures of the most stable forms of the $[H_9O_4]^+$ and $[H_{13}O_6]^+$ ions in a polar aprotic environment and to reveal the core structure of these forms; and (ii) to elucidate the effect of a counterion on the core structures and their spectroscopic features.

Since only the equilibrium solvation is considered, a detailed analysis of the proton-transfer free energy surface, and, in particular, an estimation of the potential barrier between different proton solvation structures is beyond the scope of the present study.

2. Computational Methods

B3LYP is the most popular DFT functional.[45–49] B3LYP/6-311++G** gives reasonable results for hydrogen bonds (H-bonds) formed by the first row elements.[50] It has been shown very recently, that B3LYP offers the most cost-effective choice for the prediction of the molecular vibrational properties in comparison with MP2 and hybrid density functionals M05 and M05-2X.[51] The use of the double harmonic approximation[52] allows one to obtain a quantitative or semi-qualitative description of the frequencies, relative IR intensities and Raman activities for complexes with H-bonds of different strengths in the gas phase[15,16,18,25,53] and molecular crystals.[54–58] In the present study the structures and vibrational spectra of H-bonded complexes in the gas phase and aprotic environment have been computed using Gaussian03[59] with the SCF=Tight option. An effect of the aprotic environment is taken into account in terms of the CPCM approach (acetonitrile)[60] with the radii=UAHF option. The B3LYP-PCM approximation gives reasonable description of the structures and spectroscopic properties of H-bonded systems in polar aprotic environment.[42,61–63] The minimum-energy states of the considered structures have been confirmed in the present study by calculating the harmonic frequencies scaled with a scaling factor of 0.9686.[64]

3. Results and Discussion

There are two main environmental effects on the structure and spectroscopic features of the protonated water hydrates: (i) polarization of the solvent by the hydrate dipole moment; (ii) formation of H-bonds with solvent molecules or the counterion. In the present study we separate these effects. First we consider the effect of the polarization in the terms of the CPCM approach (acetonitrile). This case corresponds to an extremely dilute solution. Then a counterion is explicitly taken into consideration. This case is somewhat closer to real experimental conditions. To avoid an appearance of contact ionic pairs between the $[H_5O_2]^+/[H_3O]^+$ cores and the counterion, only the formation of H-bonds with poor coordinating counterions, $[ClO_4]^-$ and $[BF_4]^-$, has been considered.

According to experimental[3,12–14] and theoretical[21–23,25] studies the two most stable forms of $[H_9O_4]^+$ and $[H_{13}O_6]^+$ in the gas phase can be presented as hydrated $[H_3O]^+$ and $[H_5O_2]^+$ cores. For the sake of comparison, these cores are considered separately below. Other forms of $[H_9O_4]^+$ and $[H_{13}O_6]^+$ are located well above the global-minimum structures [25] and, therefore, are not considered in the present study.

The $[H_3O]^+$core in $[H_9O_4]^+$ and $[H_{13}O_6]^+$ ions in the gas phase and acetonitrile.

The $[H_3O]^+(3H_2O)$ form of $[H_9O_4]^+$ represents the global-minimum structure of this ion, Fig. 1. In the gas-phase this form is on about 6 kJ/mol more stable than the $[H_5O_2]^+(2H_2O)$ one.[25] In acetonitrile the difference in the free energies of these two species increases further to about 9 kJ/mol. The solvent electrostatic field causes a contraction of the O1…O2-4 distances in $[H_3O]^+(3H_2O)$, Table 1. As a result, the frequencies of the O1H stretching vibrations and the bending vibration of the dangling water molecules shift to the red, while the out-of-plane bending vibration of the $[H_3O]^+$ core, $\gamma(OH_3+)$, shifts to the blue. The IR intensities of all these bands increase. The effect of the solvent polarization does not change dramatically the spectral pattern. Thus, the asymmetric O1H stretching vibrations located near 2700 cm^{-1}, that are the most IR-intensive bands of the $[H_3O]^+(3H_2O)$ form, can be further considered as the spectroscopic signature of the Eigen ion.[15,16,25]

Table 1. Selected distances (Å) and harmonic frequencies (cm^{-1}) of IR-intensive vibrations[a)] of $[H_3O]^+(3H_2O)$ and the local-minimum structure of the $[H_{13}O_6]^+$ ion[b)] in the gas phase and acetonitrile.

$[H_3O]^+(3H_2O)$			the local-minimum structure of the $[H_{13}O_6]^+$ ion[b]		
Distance[c)]/Vibration[d)]	**Gas phase**	**Acetonitrile**	**Distance/Vibration**	**Gas phase**	**Acetonitrile**
O1…O/ O1–H	2.560/ 1.012	2.549/1.018	O1…O4/O1–H4	2.619/0.998	2.588/1.007
–	–	–	O1…O2/O1–H2	2.509/1.031	2.511/1.032
–	–	–	O1…O3/O1–H3	2.512/1.029	2.512/1.032
–	–	–	ν(O3H6)	3350 (698)	3275 (2182)
–	–	–	ν(O2H5)	3337 (1113)	
ν_S(O1H)	2931 (118)	2836 (278)	ν(O1H4)[e)]	3101 (1309)	2938 (1452)
ν_{AS}(O1H)[e)]	2829 (3014)	2674 (3642)	ν_S(O1H2H3)[e)]	2634 (1648)	2559 (2380)
		2672 (3638)	ν_{AS}(O1H2H3)	2497 (4252)	2409 (4700)
$\sigma_D(OH_2)$[f)]	1583 (78)	1546 (124)	$\sigma_D(OH_2)$	1585 (100)	1546 (180)
$\gamma(OH_3+)$	1090 (376)	1166 (431)	$\gamma(OH_3+)$	1185 (278)	1233 (331)

[a)] IR intensities are given in parentheses in kM/mol;
[b)] see text for further description;
[c)] atomic numbering according to Fig. 1;
[d)] ν, σ and γ denote stretching, in-plane and out-of-plane bending vibrations, respectively;
[e)] vibration is shown in Fig. 2;
[f)] $\sigma_D(OH_2)$ denotes a bending vibration of the dangling water molecules in $[H_3O]^+(3H_2O)$;

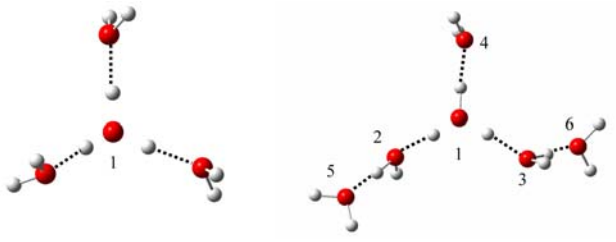

Fig 1. The structures of the $[H_3O]^+(3H_2O)$ species (left) and the local-minimum structure of the $[H_{13}O_6]^+$ ion (right) in acetonitrile. See text for further description. H-bonds are given by dotted lines. O-H covalent bonds are not shown if their lengths are above 1.01 Å.

The second solvation shell of the $[H_3O]^+$ core in $[H_{13}O_6]^+$ is asymmetric that distorts the structure of the core, Fig. 1. As a result $[H_3O]^+(5H_2O)$ is the first local-minimum structure of $[H_{13}O_6]^+$. In the gas-phase this structure is about 4 kJ/mol above the global-minimum structure that can be presented as $[H_5O_2]^+(4H_2O)$.[25] In acetonitrile the difference in the free energies of these species increases to about 8 kJ/mol. Due to the distortion the symmetry of the $[H_3O]^+$ core lowers from C_3 to C_s and the characteristic asymmetric stretching vibrations of the O1H groups disappear. Thus, this local-minimum structure can be better described as $[H_7O_3]^+(3H_2O)$. It should be noted, that $[H_7O_3]^+$ behaves as an isolated ion in weakly polar solvents (benzene and dichloroethane) in the presence of weakly basic anions (carborane counterions).[65] The distortion of the $[H_3O]^+$ core changes the nature of the most IR-intensive bands. In the $[H_7O_3]^+(3H_2O)$ form they are the bands near 2550 and 2400 cm^{-1}, that are caused by the in-phase/out-of-phase vibrations of the O1H2 and O1H3 groups, Fig. 2. These bands are accompanied by other IR-intensive bands around 3300 cm^{-1} due to other OH stretching, Table 1. Although the presence of the asymmetric second solvation shell does not effect remarkably the frequencies of the $\sigma_D(OH_2)$ bending and the $\gamma(OH_3+)$ out-of plane bending vibrations, the low IR intensities of these vibrations can hamper their experimental identification. The effect of the solvent polarization on the vibration frequencies of $[H_7O_3]^+(3H_2O)$ does not exceed 100 cm^{-1}, but the intensities of some vibrations increase strongly.

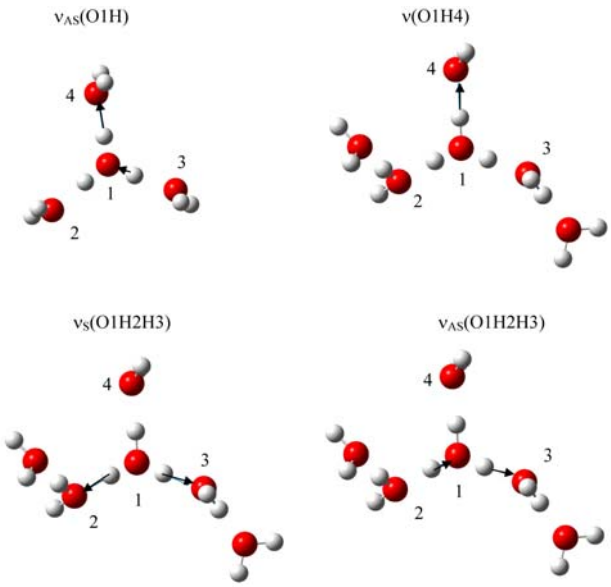

Fig. 2. Schematic representation of the normal coordinates of the ν_{AS}(O1H) stretching vibrations of the $[H_3O]^+(3H_2O)$ and the ν(O1H4), ν_S(O1H2H3), ν_{AS}(O1H2H3) stretching vibrations of the $[H_3O]^+(5H_2O)$ in acetonitrile. See text for further description. O-H covalent bonds are not shown if their lengths are above 1.01 Å.

The $[H_5O_2]^+$ core in $[H_9O_4]^+$ and $[H_{13}O_6]^+$ ions in the gas phase and acetonitrile.

The $[H_5O_2]^+(2H_2O)$ form of $[H_9O_4]^+$ is characterized by a very short inner O1…O2 H-bond, Fig. 3. The presence of the external electrostatic field resulted in an elongation of the O1…O2 distance and a contraction of the outer O1…O3, and O2…O4 distances, Table 2. While the effect of these geometrical changes on vibration frequencies is quite small, the intensities of the IR-intensive vibrations change strongly and in the opposite directions. Of special interest is the asymmetric stretching vibrations of the O1…H…O2 fragment coupled to the O1…O2 symmetric stretch. This double-band absorption is located around 900 cm^{-1} in the gas phase.[6,24,26] In acetonitrile the splitting increases and the intensity of the low-frequency band increases dramatically. This band, located near 750 cm^{-1}, together with the IR-intensive band near 1700 cm^{-1} due to the bending vibration of the water molecules of $[H_5O_2]^+$, can be regarded as the characteristic spectral pattern of the $[H_5O_2]^+(2H_2O)$ form.

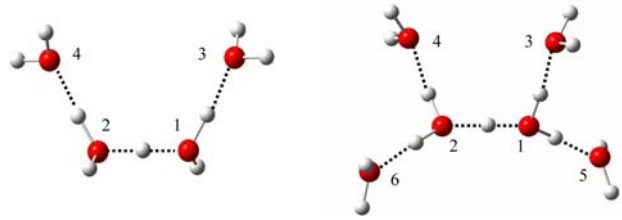

Fig 3. The structures of the $[H_5O_2]^+(2H_2O)$ (left) and $[H_5O_2]^+(4H_2O)$ (right) species in acetonitrile. H-bonds are given by dotted lines.

In contrast, in a polar environment the O…O distances between the oxygen atoms of the dangling waters and the $[H_5O_2]^+$ become quite different that breaks the symmetry of the O1-H…O2 H-bond in the core. These structural changes strongly modify the IR spectrum of the $[H_5O_2]^+(4H_2O)$, Table 2. The characteristic band corresponding to the asymmetric stretching vibrations of the O1…H…O2 fragment coupled to the O1…O2 symmetric stretch is shifted above 1100 cm^{-1} and dominates in the

Table 2. Selected distances (Å) and harmonic frequencies (cm^{-1}) of IR-intensive vibrations[a)] of $[H_5O_2]^+(2H_2O)$ and $[H_5O_2]^+(4H_2O)$ in the gas phase and acetonitrile.

Distance[b)]/	$[H_5O_2]^+(2H_2O)$		$[H_5O_2]^+(4H_2O)$	
Vibration[c)]	Gas phase	Acetonitrile	Gas phase	Acetonitrile
O1…O2/O1…H	2.389/1.195	2.396/1.198	2.392/1.196	2.408/1.132
O1…O3/O1–H3	2.591/1.004	2.580/1.009	2.674/0.988	2.625/0.998
O2…O4/O2–H4	2.592/1.004	2.580/1.009	2.674/0.988	2.685/0.988
O1…O5/O1–H5	–	–	2.679/0.988	2.626/0.998
O2…O6/O2–H6	–	–	2.679/0.988	2.687/0.988
ν(O2H) of H_5O_2+	3011 (1698)	2900 (2820)	3290 (946)	3264 (644)[d)]
			3279(1327)	3262 (1852)
ν(O1H) of H_5O_2+	2979 (1432)	2877 (976)	3278 (1180)	3097 (908)[e)]
			3253 (1216)	3056 (2563)
$\sigma(OH_2)$[f)] + σ(O1…H…O2)	1710 (1120)	1677 (610)	1713 (905)	1716 (870)
$\sigma_D(OH_2)$[f)]	1590 (170)	1558 (258)	1589 (143)	1560 (156)
σ(O1…H…O2)	1453 (175)	1458 (277)	1409 (210)	1542 (256)
				1417 (274)
ν_{AS}(O1…H…O2) + ν(O1…O2)	991 (1728)	1020 (889)	966 (2446)	1126[g)] (3513)
	829 (1905)	729 (3082)	747 (1547)	
ν(O1…O2)[h)]	–	–	–	506

[a)] IR intensities are given in parentheses in kM/mol; vibrations with the relative IR-intensities below 5% are not reported;
[b)] atomic numbering according to Fig. 3;
[c)] ν, σ and γ denote stretching, in-plane and out-of-plane bending vibrations, respectively;
[d)] stretching vibrations of the $O1H_2$ molecule;
[e)] stretching vibrations of the $O2H_2$ molecule;
[f)] $\sigma(OH_2)$ and $\sigma_D(OH_2)$ denote bending vibrations of the water molecules in $[H_5O_2]^+$ and the dangling water molecules;
[g)] "pure" asymmetric stretching vibrations of the O…H…O fragment, ν_{AS}(O…H…O).
[h)] ν(O1…O2) denotes is a Raman-active O...O stretching vibration of $[H_5O_2]^+$.

A further hydration of the $[H_5O_2]^+$ core, that is the formation of the $[H_5O_2]^+(4H_2O)$ species, does not affect remarkably the structure of the core in the gas phase. Although it leads to an elongation of the O…O distances between the core and water molecules, the spectral pattern is similar to the one of the $[H_5O_2]^+(2H_2O)$ species, Table 2. spectrum. Besides that it is worth to mention the appearance of a characteristic Raman-active line around 500 cm^{-1} (Table 2). This line is associated with the O…O stretching vibration of the $[H_5O_2]^+$ core. Raman-active lines were observed in aqueous HCl solutions[66] and $[H_5O_2]^+[ClO_4]^-$ crystals[67] at 460 and 630 cm^{-1}, respecti-

vely. These lines were tentatively assigned to the O…O stretching vibrations of $[H_5O_2]^+$.[41,68,69] Formally, a general spectroscopic feature of the $[H_5O_2]^+$ core is the frequency of the bending mode $\sigma(OH_2)$.[9,18] The position of this band depends only weakly on the asymmetry of the O…H…O fragment and the amount of water molecules solvating the $[H_5O_2]^+$ core. However, the overlapping with other vibrations can hinder its experimental identification.

According to our computations, the difference in the free energies of the global and first minimum structures of the species under this study does not exceed 10 kJ/mol. That is at least two different forms of the same protonated water hydrate can coexist in solution.

The effect of a counterion on the structure and spectral features of $[H_{13}O_6]^+$.

To reveal the effect of a counterion on the structure and spectral features of the $[H_{13}O_6]^+$ ion we have identified the low-energy forms of $[H_{13}O_6]^+[BF_4]^-$ and $[H_{13}O_6]^+[ClO_4]^-$ complexes in acetonitrile. The $[BF_4]^-$ and $[ClO_4]^-$ anions have been selected as they are big enough to prevent a strong distortion of the structure of $[H_{13}O_6]^+$ that is unavoidable in the case of point-charge anions, such as Cl^-. At the same time $[BF_4]^-$ and $[ClO_4]^-$ form stable additional H-bonds with cations.[70] Besides that these anions have been successfully used in the B3LYP-PCM computations in the past.[71]

Since the effect of both $[BF_4]^-$ and $[ClO_4]^-$ on the structure of $[H_{13}O_6]^+$ is rather the same, the numerical values obtained for the $[H_{13}O_6]^+[BF_4]^-$ complex are collected in the Supporting Information to this paper, Table S1. The presence of a counterion does not change the relative stability of the low-energy forms of $[H_{13}O_6]^+$. For both complexes the global-minimum structures are the $[H_5O_2]^+(4H_2O)$ forms. The first local-minimum structures are the $[H_7O_3]^+(3H_2O)$ forms that are 16 and 11 kJ/mol above the global-minimum structures in the case of $[BF_4]^-$ and $[ClO_4]^-$, respectively. In Fig. 4 these structures are depicted for the $[H_{13}O_6]^+[ClO_4]^-$ complex.

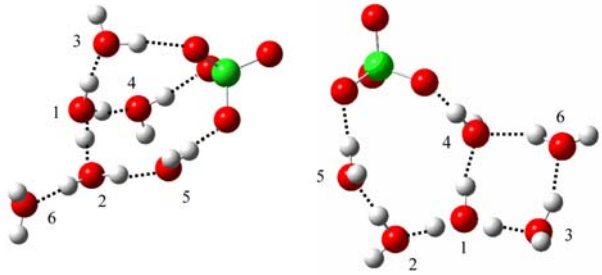

Fig. 4. The two most stable forms of $[H_{13}O_6]^+[ClO_4]^-$ complex in acetonitrile: with the $[H_5O_2]^+$ (left) and $[H_7O_3]^+$ (right) cores. H-bonds are given by dotted lines. O-H covalent bonds are not shown if their lengths are above 1.01 Å.

Table 3. Selected O…O distances (Å) and frequencies (cm^{-1}) of the IR-intensive vibrations[a] of the two low-energy forms[b] of $[H_{13}O_6]^+[ClO_4]^-$ in acetonitrile.

$[H_5O_2]^+(4H_2O)[ClO_4]^-$		$[H_7O_3]^+(3H_2O)[ClO_4]^-$	
Distance[b]/Vibration[c]	**Computed value**	**Distance[b]/Vibration[c]**	**Computed value**
O1…O2/O1…H	2.447/1.083	O1…O2/O1–H2	2.490/1.046
O1…O3/O1–H3	2.586/1.011	O1…O3/O1–H3	2.532/1.031
O1…O4/O1–H4	2.591/1.011	O1…O4/O1–H4	2.617/1.006
O2…O5/O2–H5	2.700/0.988	O2…O5/O2–H5	2.645/0.996
O2…O6/O2–H6	2.725/0.983	O3…O6/O3–H6	2.691/0.988
ν_S(O1H)	2917 (1210)	ν(O1H4)[d]	2941 (1421)
ν_{AS}(O1H)	2798 (2210)	ν_S(O1H)[d]	2544 (2023)
		ν_S(O1H)	2243 (4449)
ν_{AS}(O…H…O)	1812 (3096)		
$\sigma(OH_2)$[e] + ν_{AS}(O…H…O)	1708 (146)		
$\sigma(OH_2)$ + σ(O…H…O)	1670 (600)		
$\sigma_D(OH_2)$[f]	1590 (364)		
σ(O…H…O) + $\sigma(OH_2)$	1399 (344)	γ(O1H_3+)	1264 (346)
σ(O…H…O) + Torsion[e]	896 (577)		
Torsion	654 (200)		
ν(O…O)[g]	420		

[a] IR intensities are given in parentheses in kM/mol; vibrations with the relative IR-intensities below 3% are not reported;
[b] structure and atomic numbering according to Fig. 4;
[c] ν, σ and γ denote stretching, in-plane and out-of-plane bending vibrations, respectively;
[d] vibration is shown in Fig. 2;
[e] $\sigma(OH_2)$ denotes a bending vibration of the water molecules in the $[H_5O_2]^+$ core;
[f] $\sigma_D(OH_2)$ denotes a bending vibration of the dangling water molecules;
[g] ν(O…O) denotes a Raman-active O...O stretching vibration of $[H_5O_2]^+$.

The characteristic spectral features of the "bare" $[H_5O_2]^+(4H_2O)$ form are the IR-intensive bands of a mixed mode near 1100 cm^{-1} that includes the asymmetric stretching vibration of the O1…H…O2 fragment, the IR-intensive band near 1700 cm^{-1} corresponding to the bending vibration of the water molecules of $[H_5O_2]^+$ and the Raman-active band near 500 cm^{-1}, Table 2. The anion dramatically affects the mutual orientation of the water molecules, but the $[H_5O_2]^+$ core remains well-defined. In the presence of $[ClO_4]^-$ the O1…O2 distance in the core increases, that removes the coupling of other vibrations to the asymmetric stretching vibration of the O1…H…O2 fragment and causes a strong blue shift of the latter up to 1800 cm^{-1}, Table 3. In contrast, the OH-vibrations shift to the red down to 2900 and 2800 cm^{-1}. The O1…O2 stretching remains Raman-active, a line at 420 cm^{-1}. However, this band hardly can be used to identify the $[H_5O_2]^+$ core, because a large number of other Raman-active bands associated with counterion vibrations appears in the same frequency region.

The characteristic spectral features of the "bare" $[H_7O_3]^+(3H_2O)$ form are the IR-intensive bands near 2600/2450 cm^{-1} and 3300 cm^{-1} due to the (O1H) and other OH stretching vibrations, respectively. In the presence of a counterion the $[H_7O_3]^+$ core is distorted and does not exist as a well-defined unit. The first local-minimum structure of the $[H_{13}O_6]^+[ClO_4]^-$ complexes can be characterized by the three IR-intensive bands in the 2200–3000 frequency region. Since other protonated water hydrates do not exhibit in acetonitrile any IR-intensive bands in the 2600–2200 frequency region, the bands near 2550 and 2250 cm^{-1} can be considered as a characteristic spectral features of this complex.

Recently, vibrations of the $[H_{13}O_6]^+[ClO_4]^-$ complex have been studied in depth experimentally.[10] Observed band at 2855, 1747, 1198, and 672 cm^{-1} were tentatively assigned to a ν(OH) stretching vibrations of $[H_5O_2]^+$, an in-plane bending vibration of $[H_5O_2]^+$, an asymmetric stretching vibrations of the O1…H…O2 fragment, and a torsion vibration, respectively. These data provide us opportunity to inspect the feasibility of the B3LYP-PCM approximation to predict correctly spectroscopic features in the condense phase. According to this approximation the global-minimum structure of the $[H_{13}O_6]^+[ClO_4]^-$ complex is indeed characterized by the symmetric and asymmetric stretching vibrations of $[H_5O_2]^+$ at 2917 and 2798 cm^{-1}, respectively; and the torsion vibration at 654 cm^{-1}, Table 3. The agreement with the experimentally observed values is reasonable. Our computational modeling reveals that the attribution of the experimental bands at 1747 and 1198 cm^{-1} in[10] is questionable. Indeed, the shortest O…O distance in the $[H_{13}O_6]^+$ ion is about 2.5 Å, Table 3 and Fig. 8 in Ref. 10. According to the available correlation between the hydrogen bond geometry and the OH stretching frequency, for the O…O distance of 2.5 Å one expects the asymmetric stretching vibration of the O…H…O fragment around 2000 cm^{-1}.[72, 73] The theoretical value of 1812 cm^{-1} is again very close to the experimental one. On the other hand, the considered correlation is characterized by a large dispersion for short H-bonds, e.g. see Fig. 1 in Ref. 74. This is why the experimental band at 1747 cm^{-1} can be assigned to the asymmetric stretching vibrations of the O1…H…O2 fragment. The attribution of the experimental band at 1198 cm^{-1} is more problematic. The band at 1200 cm^{-1} can be assigned to valence vibrations of the counterion strongly coupled to the torsion vibration of the dangling water molecules of $[H_{13}O_6]^+$. This coupling can explain the strong H/D isotope effect on the vibration frequency.[10] There are a number of IR-intensive vibrations of the $[BF_4]^-$ and $[ClO_4]^-$ species below 1200 cm^{-1}. These vibrations are not reported as they are counterion specific and their analysis is beyond the scope of the present study. However, a more realistic alternative is that in some $[H_{13}O_6]^+$ $[ClO_4]^-$ clusters the specific interaction between the cation and anion is lost, and the $[H_{13}O_6]^+$ cation presents in the "bare" $[H_5O_2]^+$ $(4H_2O)$ form. The dissociation of a bulky cation and $[BF_4]^-$ in an aprotic polar solvent has been demonstrated experimentally.[70] An isolated $[H_5O_2]^+(4H_2O)$ is characterized by a very intensive band at 1100–1200 cm^{-1} due to a mixed mode that includes the asymmetric stretching vibration of the O1…H…O2 fragment, Table 2. Thus, even if this form is present in a small amount, it can be detected experimentally.

According to the B3LYP-PCM computations, the difference in the free energies of the most stable $[H_5O_2]^+(4H_2O)$ structure and the next stable structure $[H_7O_3]^+(3H_2O)$ should be to small to exclude a dynamic equilibrium between these two structures in solution. A question arises whether $[H_7O_3]^+(3H_2O)$ can be identified. The problem is that species containing either $[H_3O]^+$ or $[H_7O_3]^+$ cores are characterized by the only characteristic band located in the spectral region between 2800 and 2400 cm^{-1}. A closer look on experimental spectra reported in[10] allows one to argue that there are some spectral features in this region, those are however not clearly pronounced. Thus, the presence of such species in solution cannot be neither excluded nor proved. In any case the $[H_3O]^+$ or $[H_7O_3]^+$ cores based structures do not dominate at that conditions.

Special attention should be paid to the geometrical criteria used in the first-principle MD simulation studies for identification of the $[H_3O]^+$, $[H_5O_2]^+$ and $[H_7O_3]^+$ cores. The condition R(O…O) < 2.45 Å is sufficient for the identification of the $[H_5O_2]^+$ core.[29,31,32] The geometrical criterion for the discrimination between the $[H_3O]^+$ and $[H_7O_3]^+$ cores is not obvious. For example, in Ref. 75 the $[H_3O]^+$ core was identified when an oxygen atom was within 1.3 Å of three hydrogen atoms. According to Tables 1, 2, and 3, all three cores fit to this criterion.

In the present study the effects of mechanical anharmonicity were not taken into account. Reasonable agreement between the experimental and theoretical frequencies, computed in the double-harmonic approximation may be due to the consolation of errors. According to Ref. 76, the harmonic frequency of the asymmetric stretching vibration of the O1…H…O2 fragment of $H_5O_2^+$ may be close to the experimental value, because the anharmonic correction causes an up-shift of this frequency, while the coupling with the O1…O2 symmetric stretch is responsible for a down-shift.

4. Conclusions

In the present study we have identified the spectroscopic signatures of the most stable forms of $[H_9O_4]^+$ and $[H_{13}O_6]^+$ ions in a polar aprotic environment and revealed the core structure of these forms. Formally, these structures can be presented as hydrated $[H_3O]^+$ and $[H_5O_2]^+$ cores. The effect of the polarization of the aprotic media on the structure and spectral features of the $[H_3O]^+$ core strongly depends on the symmetry of the hydration shell. For $[H_9O_4]^+$ in acetonitrile the structure with the $[H_3O]^+$ core remains the most stable one and can be easily identified by the IR-intensive band around 2700 cm^{-1} due to the OH stretching vibrations of $[H_3O]^+$. By contrast, the distortion of the $[H_3O]^+$ core in $[H_{13}O_6]^+$ in acetonitrile is so strong, that it should be better described as the $[H_7O_3]^+$ core. The characteristic spectral pattern of this form are two bands near 2550 and 2400 cm^{-1} due to the in-phase/out-of-phase vibrations of two central OH groups. The effect of the polarization on the structure and spectral features of the $[H_5O_2]^+$ core is pronounced much smaller. In all cases the $[H_5O_2]^+$ core based structures are characterized by a very intensive band or a pair of bands in the spectral region between 700 and 1200 cm^{-1} due to mixed modes that include the asymmetric stretching vibration of the central O…H…O fragment.

Taking into account the effect of the solvent polarization on the structure of $[H_3O]^+$ and $[H_5O_2]^+$ core bases species, it becomes obvious that interactions with a counterion will result in a dramatic distortion of any $[H_3O]^+$ core species and the lost of the core specificity. In other words, the Eigen cation cannot be a useful model unit whose spectral features can help to interpret the experimental spectral pattern in the presence of a counterion. In contrast, the $[H_5O_2]^+$ core remains identifiable even when the $[H_{13}O_6]^+$ hydrate is involved in specific interactions with a bulky counterion. The $[H_5O_2]^+$ core is characterized by the short O…O distance (< 2.45 Å), IR-intensive band near 1720 cm^{-1} and Raman-active line around 500 cm^{-1}. The agreement between the experimental and computed values of the characteristic vibrations is reasonable and has allowed us to correct the attribution of some of these vibration reported in the past.

5. Acknowledgements

This study was supported by the Russian Foundation for Basic Research (09-03-91336, 11-03-00235 and 11-03-00583) and the German Academic Exchange Service (DAAD) in the framework of the German-Russian Interdisciplinary Science Center (G-RISC).

Supporting Information Available. Computed values of the selected O…O distances and frequencies of the IR-intensive vibrations of the two low-energy forms of $[H_{13}O_6]^+[BF_4]^-$ in acetonitrile (Suppl.pdf).

6. References

1. G. V. Yukhnevich, E. G. Tarakanova, V. D. Maiorov and N. B. Librovich, *Usp. Khim.* **1995**, *64*, 901–911 and references therein.
2. G. Zundel, *Adv. Chem. Phys*. **2000**, *111*, 1–217.
3. H.-C. Chang, C.-C. Wu, J.-L. Kuo, *Int. Rev. Phys. Chem.* **2005**, *24*, 553–578.
4. D. Marx, *ChemPhysChem* **2006**, *7*, 1848–1870.
5. G. A. Voth, *Acc. Chem. Res*. **2006**, *39*, 143–150.
6. O. Vendrell, H.-D. Meyer, *Phys. Chem. Chem. Phys*. **2008**, *10*, 4692–4703.
7. M. V. Vener, X. Radzanska, J. Sauer, *Phys. Chem. Chem. Phys*. **2009**, *11*, 1702–1712.
8. J. M. J. Swanson and J. Simons, *J. Phys. Chem. B* **2009**, *113*, 5149–5161.
9. M. V. Vener, N. B. Librovich, *Int. Rev. Phys. Chem*. **2009**, *28*, 407–434.
10. E. S. Stoyanov, I. V. Stoyanova, C. A. Reed, *Chem. Sci*. **2011**, *2*, 462–472.
11. G. A. Luduena, T. D. Kühne and D. Sebastiani, *Chem. Mater.* **2011**, *23,* 1424–1429.
12. Y. K. Lau, S. Ikuta, P. Kebarle, *J. Amer. Chem. Soc*. **1982**, *104*, 1462–1469.
13. J.-C. Jiang, Y.-S. Wang, H.-C. Chang, S. H. Lin, Y. T. Lee, G. Niedner-Schatteburg, *J. Am. Chem. Soc.* **2000**, *122*, 1398–1410.
14. K. R. Asmis, N. L. Pivonka, G. Santambrogio, M. Brümmer, C. Kaposta, D. M. Neumark, L. Wöste*, Sci*. **2003**, *299*, 1375–1377.
15. J. M. Headrick, E. G. Diken, R. S. Walters, N. I. Hammer, R. A. Christie, J. Cui, E. M. Myshakin, M. A. Duncan, M. A. Johnson, K. D. Jordan, *Sci.* **2005**, *308*, 1765–1768.
16. N. I. Hammer, E. G. Diken, J. R. Roscioli, M. A. Johnson, E. M. Myshakin, K. D. Jordan, A. B. McCoy, X. Huang, J. M. Bowman, S. Carter, *J. Chem. Phys.* **2005**, *122*, 24430
17. K. Mizuse, A. Fujii, N. Mikami, *J. Chem. Phys*. **2007**, *126*, 231101.
18. L. R. McCunn, J. R. Roscioli, M. A. Johnson and A. B. McCoy, *J. Phys. Chem. B* **2008**, *112*, 321–327.
19. H.-H. Limbach, P. M. Tolstoy, N. Pérez-Hernández, J. Guo, I. G. Shenderovich, G. S. Denisov, *Israel J. Chem.* **2009**, *49*, 199–216.

20. Y. Kim, Y. Kim, *Chem. Phys. Lett*. **2002**, *362*, 419–427.
21. M. Śmiechowski, J. Stangret, *J. Chem. Phys.* **2006**, *125*, 204508.
22. I. Shin, M. Park, S. K. Min, E. C. Lee, S. B. Suh, K. S. Kim, *J. Chem. Phys.* **2006**, *125*, 234305.
23. M. Park, I. Shin, N. J. Singh, and K. S. Kim, *J. Phys. Chem. A* **2007,** *111*, 10692–10702.
24. O. Vendrell, F. Gatti, H.-D. Meyer, *Angew. Chem. Int. Ed*. **2007**, *46*, 6918–6921.
25. M. Jieli and M. Aida, *J. Phys. Chem. A* **2009**, *113*, 1586–1594.
26. O. Vendrell, F. Gatti, H.-D. Meyer, *Angew. Chem. Int. Ed*. **2009**, ***48***, 352–355.
27. C. Lao-ngam, P. Asawakun, S. Wannarat, K. Sagarik, *Phys. Chem. Chem. Phys*. **2011**, *13*, 4562–4575.
28. F. Agostini, R. Vuilleumier, G. Ciccotti, *J. Chem. Phys*. **2011**, *134*, 0843020.
29. M. Tuckerman, K. Laasonen, M. Sprik and M. Parrinello, *J. Chem. Phys*. **1995**, *103*, 150–161.
30. R. Vuilleumier and D. Borgis, *J. Chem. Phys*. **1999**, *111*, 4251–4266.
31. J. Kim, U. W. Schmitt, J. A. Gruetzmacher, G. A. Voth and N. E. Scherer, *J. Chem. Phys*. **2002**, *116*, 737–746.
32. A. J. Sillanpää, K. Laasonen, *Phys. Chem. Chem. Phys*. **2004**, *6*, 555–565.
33. D. Asthagiri, L. R. Pratt and J. D. Kress, *Proc. Natl. Acad. Sci. U.S.A.* **2005,** *102*, 6704–6708.
34. A. Botti, F. Bruni, M. A. Ricci, A. K. Soper, *J. Chem. Phys*. **2006**, *125*, 014508.
35. J.M. Heuft, E. Meijer, *Phys. Chem. Chem. Phys*. **2006**, *8*, 3116–3123.
36. T. Murakhtina, J. Heuft, E. J. Meijer and D. Sebastiani, *Chem Phys Chem* **2006**, *7*, 2578–2584.
37. O. Markovitch, H. Chen, S. Izvekov, F. Paesani, G. A. Voth and N. Agmon, *J. Phys. Chem. B* **2008,** *112*, 9456–9466.
38. H. Takahashi, H. Ohno, T. Yamauchi, R. Kishi, S. Furukawa, M. Nakano, and N. Matubayasi, *J. Chem. Phys.* **2008**, *128*, 064507.
39. V. Bush, A. Dubrovskiy, F. Mohamed, M. Parrinello, J. Sadlej, A. D. Hammerich and J. P. Devlin, *J. Phys. Chem. A* **2008**, *112*, 2144–2161.
40. C. M. Maupin, B. Aradi, G. A. Voth, *J. Phys. Chem. B* **2010**, *114*, 6922–6931.
41. M.V. Vener, J. Sauer, *Phys. Chem. Chem. Phys*. **2005**, *7***,** 258–263.
42. S. Kong, I. G. Shenderovich, M. V. Vener, *J. Phys. Chem. A* **2010**, *114*, 2393–2399.
43. D. Mauder, D. Akcakayiran, S. B. Lesnichin, G. H. Findenegg, I. G. Shenderovich, *J. Phys. Chem. C* **2009**, *113*, 19185–19192.
44. Y. J. Lee, B. Bingöl, T. Murakhtina, D. Sebastiani, W. H. Meyer, G. Wegner and H. W. Spiess, *J. Phys. Chem. B* **2007**, *111*, 9711–9721.
45. C. F. Sousa, P. A. Fernandes, M. J. Ramos, *J. Phys. Chem. A* **2007**, *111*, 10439–10452.
46. H. Szatyłowicz, T. M. Krygowski, J. E. Zachara-Horeglad, *J. Chem. Inf. Mod.* **2007**, *47*, 875–886.
47. J. Stare, J. Panek, J. Eckert, J. Grdadolnik, J. Mavri, D. Hadzi, *J. Phys. Chem. A* **2008**; *112*, 1576–1586.
48. R. Borstnar, A. R. Choudhury, J. Stare, M. Novic, J. Mavri, *J. Mol. Struct.-THEOCHEM* **2010**, *947*, 76–82.
49. D. J. O'Leary, D. D. Hickstein, B. K. V. Hansen, P. E. Hansen, *J. Org. Chem*. **2010**, *75*, 1331–1342.
50. W. Koch, M.C. Holthausen, A Chemist's guide to density functional theory, Wiley-VCH, Weinheim, Germany, **2001**, pp. 1–300.
51. E. E. Zvereva, A. R. Shagidullin, S. A. Katsyuba, *J. Phys. Chem. A* **2011**; *115*, 63–69.
52. E. F. Valeev, H. F. Schaefer, *J. Chem. Phys*. **1998**, *108*, 7197–7201.
53. H. M. Lee, A. Kumar, M. Kołaski, D. Y. Kim, E. C. Lee, S. K. Min, M. Park, Y. C. Choi, K. S. Kim, *Phys. Chem. Chem. Phys.* **2010**, *12*, 6278–6287.
54. M. V. Vener, A. V. Manaev, V. G. Tsirelson, *J. Phys. Chem. A* **2008,** *112*, 13628–13632.
55. L. Valenzano, A. Meyer, R. Demichelis, B. Civalleri, R. Dovesi, *Phys. Chem. Minerals* **2009**, *36*, 415–420.
56. M. D. King, T. M. Korte, *J. Phys. Chem. A* **2010**, *114,* 7127–7138.
57. M. R. Hudson, D. G. Allis, B. S. Hudson, *J. Phys. Chem. A* **2010,** *114,* 3630–3641.
58. M. V. Vener, A. N. Egorova, V. G. Tsirelson. *Chem. Phys. Lett.* **2010**, *500,* 272–276.
59. M. J. Frisch, G. W. Trucks, H. B. Schlegel et al. Gaussian 03, Resivion D.01, Gaussian, Inc., Wallingford, CT, **2004**.
60. V. Barone, M. Cossi, *J. Phys. Chem. A*, **1998**, *102*, 1995–2001.
61. A. Panuszko, E. Gojło, J. Zielkiewicz, M. Sämiechowski, J. Krakowiak, J. Stangret, *J. Phys. Chem. B* **2008,** *112,* 2483–2493.
62. A. Filarowski, A. Koll, P. E. Hansen, M. Kluba, *J. Phys. Chem. A* **2008**, *112,* 3478–2485.
63. M. Shanmugasundaram, M. Puranik, *Phys. Chem. Chem. Phys*. **2011**, *13*, 3851–3862
64. J. P. Merrick, D. Moran, L. Radom, *J. Phys. Chem. A* **2007**, *111*, 11683–11700.
65. E. S. Stoyanov, I. V. Stoyanova, F. S. Tham, C. A. Reed, *J. Am. Chem. Soc.* **2008**, *130*, 12128–12138.
66. N. B. Librovich, V. P. Sakun, N.D. Sokolov, *Chem. Phys*. **1981**, *60*, 425–426.
67. A. C. Pavia, P. A. Giguère, *J. Chem. Phys*. **1970**, *52*, 3551–3554.
68. J. B. Bates, L. M. Toth, *J. Chem. Phys*. **1974**, *61*, 129–137.
69. D. J. Jones, J. Roziere, J. Penfold, J. Tomkinson, *J. Mol. Struct*. **1989**, *195*, 283–291.
70. S. B. Lesnichin, P. M. Tolstoy, H.-H. Limbach, I. G. Shenderovich, *Phys. Chem. Chem. Phys.* **2010**, *12*, 10373–10379.
71. V. A. Nikitina, R. R. Nazmutdinov, G. A. Tsirlina, *J. Phys. Chem. B* **2011,** *115,* 668–677.
72. A. Novak. *Struct. Bonding* **1974**, *18*, 177–201.

73. T. Steiner, *Angew. Chem. Int. Ed.* **2002**, *41*, 48–76.
74. N. D. Sokolov, M. V. Vener, V. A. Savel'ev, *J. Mol. Struct*. **1990**, *222*, 365–386.
75. Y.-K. Choe, E. Tsuchida, T. Ikeshoji, S. Yamakawa, S. Hyodo, *Phys. Chem. Chem. Phys.* **2009**, *11*, 3892–3899.
76. M. V. Vener, J. Sauer, *Chem. Phys. Lett*. **1999**, *312*, 591–597.

Povzetek

S kvantno kemijsko metodo B3LYP in polarizabilnim kontinuirnim modelom topila smo proučevali najbolj obstojne strukture ionov $[H_9O_4]^+$ in $[H_{13}O_6]^+$ v acetonitrilni raztopini, njihove relativne stabilnosti ter infrardeče (IR) in Ramanske spektre. Osrednji del struktur sta zvrsti $[H_3O]^+$ oziroma $[H_5O_2]^+$, obdani z molekulami vode. Študirali smo dva vpliva okolice na spektroskopske lastnosti protoniranih vodnih hidratov: (i) polarizacijo topila z dipolnim momentom hidrata in (ii) tvorbo vodikovih vezi z velikimi protiioni (ClO_4^- in BF_4^-). Vpliv polarizacije na strukturo zvrsti $[H_3O]^+$ je močno odvisen od simetrije hidratacijskega ovoja. Popačenje hidratiranega $[H_3O]^+$ vodi v spremembo strukture v $[H_7O_3]^+$, kar se pozna na najbolj intenzivnih trakovih v Ramanskem spektru. Zaradi občutljivosti sredice $[H_3O]^+$ na spremembe v okolici je njena identifikacija težka. Nasprotno temu je sredica $[H_5O_2]^+$ manj občutljiva na popačitve, njene značilnosti – zelo kratka razdalja O...O (< 2.45 Å), IR trak pri 1720 cm^{-1} ter Ramanski trak pri 500 cm^{-1} – se ohranijo tudi pri specifični interakciji z velikimi protiioni. V članku razpravljamo tudi o geometrijskih kriterijih za identifikacijo sredic $[H_3O]^+$, $[H_5O_2]^+$ in $[H_7O_3]^+$.